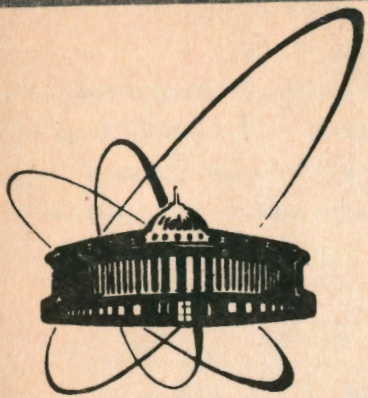

объединенный
институт
ядерных
исследований
дубна

E4-92-54

G.G.Adamian*, N.V.Antonenko, R.V.Jolos,
A.K.Nasirov*

# MICROSCOPIC DRIVING POTENTIAL FOR A DINUCLEAR SYSTEM

Submitted to "Nuclear Physics A"

1992

Адамян Г.Г. и др.
E4-92-54

Микроскопический driving потенциал
для двойной ядерной системы

Предложен метод построения driving потенциала для двойной ядерной системы в рамках микроскопического подхода. Используется феноменологическое соотношение между транспортными коэффициентами и driving потенциалом. Результаты расчетов показали удивительное сходство микроскопического и феноменологического driving потенциалов, что является дополнительным подтверждением справедливости микроскопического подхода.

Работа выполнена в Лаборатории теоретической физики ОИЯИ.

Препринт Объединенного института ядерных исследований. Дубна 1992

---

Adamian G.G. et al.
E4-92-54

Microscopic Driving Potential
for a Dinuclear System

A method is proposed to derive the driving potential for a dinuclear system within microscopic approach. The phenomenological ratio between the transport coefficients and driving potential is used. The calculated results have demonstrated surprising likeness of the microscopic and phenomenological driving potentials. This is the further argument for the validity of the microscopic approach.

The investigation has been performed at the Laboratory of Theoretical Physics, JINR.

Preprint of the Joint Institute for Nuclear Research. Dubna 1992

## 1. Introduction

The time evolution of a dinuclear system is described usually in the framework of the transport model. In this approach the time dependence of the probability $P_{Z(A)}(t)$ to find a system at the moment $t$ in the state with the charge (mass) asymmetry $Z(A)$ is described by the master equation

$$\begin{aligned}\frac{\partial P_{Z(A)}(t)}{\partial t} &= \Delta^{(-)}_{Z+1(A+1)} P_{Z+1(A+1)}(t) + \Delta^{(+)}_{Z-1(A-1)} P_{Z-1(A-1)}(t) \\ &- (\Delta^{(+)}_{Z(A)} + \Delta^{(-)}_{Z(A)}) P_{Z(A)}(t). \end{aligned} \tag{1}$$

Transport coefficients $\Delta^{(\pm)}_{Z(A)}$ characterize the probability of the nucleon transfer from a heavy to a light nucleus ($\Delta^{(+)}_{Z(A)}$) or in the opposite direction ($\Delta^{(-)}_{Z(A)}$). To simplify the notation in the following, we will write $Z$ instead of $Z(A)$ having in mind that charge and mass evolutions are described analogously. In [1]) the following parameterization has been suggested for the transport coefficients

$$\begin{aligned}\Delta^{(-)}_{Z(A)} &= s_0 \exp\{[U(Z) - U(Z-1)]/2\tau\}, \\ \Delta^{(+)}_{Z(A)} &= s_0 \exp\{[U(Z) - U(Z+1)]/2\tau\}. \end{aligned} \tag{2}$$

Here $s_0$ is a constant characterizing the time scale, $\tau$ is the temperature of the dinuclear system which can be expressed through the excitation energy of the system $E^*_l$ in the Fermi gas approximation by the expression $\tau = \sqrt{E^*_l/a}$ where $a = (A_P + A_T)/8$ MeV. Here $A_P$ and $A_T$ are the mass numbers of the light and heavy fragment. The excitation energy $E^*_l$ depends on the kinetic energy of the projectile and the orbital momentum $l$ of collision. The potential energy of the dinuclear system $U(Z)$ which is a function of the light fragment charge $Z$ completely determines the evolution direction depending on the position of the injection point with respect to the Businaro-Gallone maximum.

The parameterization (2) uses the macroscopic characteristics of the system. In the phenomenological models the potential energy is taken as a sum of the liquid drop energy, the shell correction term which decreases with increasing the excitation energy and the nucleus-nucleus interaction energy,

$$U(Z) = U_{LD}(Z) + U_{SH}(Z)\exp(-E^*_l/E_0) + U_{int}(Z,R). \tag{3}$$

The parameter $E_0$ characterizes the exponential decrease of the shell correction term with increasing the excitation energy $E^*_l$. The nucleus-nucleus interaction potential $U_{int}(Z,R)$ includes the Coulomb and the nuclear terms. The nuclear part of $U_{int}(Z,R)$

can be taken in the well known proximity form [2]). Hear $R$ is the distance between the centers of interacting nuclei. For heavy systems and the small values of $l$ the influence of the rotational energy is negligible [3]).

The dependence of the macroscopic nucleon transition probabilities $\Delta_Z^{(\pm)}$ on $Z$ is determined under the assumption that the nucleon can be transferred into any single particle state favoured by the energy conservation. In this approach, the shell effects are included into $\Delta_Z^{(\pm)}$ only through the nucleon separation energies. The structure of the single particle spectra is not taken into account although it is known from the experimental data that it plays an important role in some cases. For instance, in the charge and mass distributions of the reaction products there are local maxima corresponding to the closed shell nuclei [4,5]). Based on the knowledge of the potential energy surface it is not always possible to explain the increased production of the light nuclei $^4$He, $^{12}$C, $^{15}$N and $^{16}$O in deep inelastic heavy ion collisions. It means that during the collision the individual properties of the colliding nuclei are conserved and the shell effect plays an essential role. For this reason only the microscopic approach can be used as a basis to treat these effects.

## 2. Microscopic calculations of the driving potential

The main ingredients of the microscopic model of deep inelastic collisions are the realistic single particle level scheme, nucleon separation energy, single particle matrix elements of nucleon transfer under the action of the mean field of the reaction partner and the effective residual forces. The strength of the effective forces determines the characteristic time of the intrinsic excitation energy termalization. Up to now we did not take into account the residual forces directly but effectively included their action into consideration introducing the temperature-dependent occupation numbers.

The microscopically determined transition probabilities $\tilde{\Delta}_Z^{(\pm)}$ [6,7]) are

$$\tilde{\Delta}_Z^{(+)} = \frac{1}{\Delta t}\sum_{P,T}|g_{PT}^Z(R)|^2\, n_T^Z(\tau)\,(1-n_P^Z(\tau))\,\frac{\sin^2\left(\frac{\Delta t}{2\hbar}\left[\tilde{E}_P^Z-\tilde{E}_T^Z\right]\right)}{\left(\tilde{E}_P^Z-\tilde{E}_T^Z\right)^2/4},$$

$$\tilde{\Delta}_Z^{(-)} = \frac{1}{\Delta t}\sum_{P,T}|g_{PT}^Z(R)|^2\, n_P^Z(\tau)\,(1-n_T^Z(\tau))\,\frac{\sin^2\left(\frac{\Delta t}{2\hbar}\left[\tilde{E}_P^Z-\tilde{E}_T^Z\right]\right)}{\left(\tilde{E}_P^Z-\tilde{E}_T^Z\right)^2/4}. \qquad (4)$$

Here $P$ and $T$ are the quantum numbers characterizing the single particle states in light and heavy nuclei respectively, $n_P(n_T)$ are the temperature dependent occupation



numbers of the single particle states in light (heavy) nucleus, $g_{PT}$ are the proton transition matrix elements. The time interval $\Delta t$ must be larger than the relaxation time of the mean field but considerably smaller than the characteristic evolution time of the macroscopic quantities. The mutual influence of the mean fields of the reaction partners leads to the renormalization of the single particle energies $E_{P(T)}$ of noninteracting nuclei. Due to the long range character the Coulomb interaction gives the main contribution to this renormalization. Thus, for protons approximately

$$\tilde{E}_{P(T)}^Z = E_{P(T)} + Z_{T(P)}e^2/2R,$$

where $Z_{P(T)}$ is the atomic number of a light (heavy) fragment. As was shown in [8]) the Coulomb interaction increases the formation probability of the very asymmetric configurations.

Peculiarities of the structure of interacting nuclei are taken into account explicitly in transport coefficients $\tilde{\Delta}_Z^{(\pm)}$. These peculiarities influence the dinuclear system evolution. Thanks to the selection rules for the projection of spin and single particle momentum, the existence of the nuclear shell structure restricts essentially the probability of nucleon transfer. Because of the weak overlapping of the wave functions the transitions between the single particle levels near the Fermi surfaces of the interacting nuclei can be made weaker by these selection rules. This fact indicates more wide possibilities for the description of the dinuclear system dynamics within microscopic approach.

Let the phenomenological expressions (2) for transport coefficients be valid. Then we can equate expressions (2) and (4) and obtain the following iteration procedure for reconstruction of the microscopic driving potential.

$$\tilde{U}(Z+1) = \tilde{U}(Z) + 2\tau\ln\left(\frac{\tilde{\Delta}_Z^{(-)}}{s_0}\right), \qquad (5)$$

$$\tilde{U}(Z-1) = \tilde{U}(Z) + 2\tau\ln\left(\frac{\tilde{\Delta}_Z^{(+)}}{s_0}\right). \qquad (6)$$

Using (5) and (6) we can obtain the formula without the free parameter $s_0$.

$$\tilde{U}(Z+1) = \tilde{U}(Z) + \tau\ln\left(\frac{\tilde{\Delta}_{Z+1}^{(-)}}{\tilde{\Delta}_Z^{(+)}}\right). \qquad (7)$$

Since the phenomenological model describes the charge and mass distributions for many reactions quite well, it is interesting to compare the macroscopic driving potential with the microscopic calculated driving potential.

## 3. Calculation results

Let us compare the calculated microscopic driving potential with the driving potential used in the phenomenological models. For instance, we consider the dinuclear system with $Z_{tot} = 108$. This dinuclear system is formed in the reactions $^{40}$Ar(220MeV)+$^{232}$Th and $^{32}$S(192MeV)+$^{238}$U which give the near compound nuclei with the same excitation energy ($E_l^* = 34$ MeV). However the charge (mass) distributions of these reactions are qualitatively different [3,9]).

For the calculation of the transport coefficients $\tilde{\Delta}_Z^{(\pm)}$ (4) we use the realistic single particle level schemes. The absolute values of the single particle energies have been determined in agreement with experimental nucleon separation energies.

The matrix elements $g_{PT}(R)$ are taken from [10]), where the analytical method of their calculation has been suggested. This method allows one to obtain matrix elements for various values of $R$. At $R \geq R_{E_P} + R_{E_T}$ ($R_{E_{P(T)}}$ is the radius of sewing for internal and external parts of the single particle state $P(T)$) we have

$$g_{PT}(R) = (-1)^{l_T+m_T+1/2} C^{ex}_{l_T} C^{ex}_{l_P} \sqrt{(2j_P+1)(2j_T+1)}$$
$$\times \sum_L (j_T - \tfrac{1}{2}, j_P \tfrac{1}{2} | L0)\,(j_T - m_T, j_P m_P | L0)\,[A_P k_L(æ_P R) + A_T k_L(æ_T R)]\,. \qquad (8)$$

At $R < R_{E_P} + R_{E_T}$ the following expression has to be used

$$g_{PT}(R) = (-1)^{l_T+m_T+1/2} C^{ex}_{l_T} C^{ex}_{l_P} \sqrt{(2j_P+1)(2j_T+1)}$$
$$\times \sum_L (j_T - \tfrac{1}{2}, j_P \tfrac{1}{2} | L0)\,(j_T - m_T, j_P m_P | L0)$$
$$\times \{(-1)^{(L-l_T-l_P)/2} [B_P y_L(\kappa_P R) + B_T y_L(\kappa_T R) + D_P j_L(\kappa_P R) + + D_T j_L(\kappa_T R)]$$
$$+ G_P k_L(æ_P R) + G_T k_L(æ_T R) + I^0_{PT}(R, L)\}\,. \qquad (9)$$

Here $j_L(x)$, $i_L(x)$, $k_L(x)$, $y_L(x)$ are the spherical Bessel functions [11]), $l_{P(T)}$ and $j_{P(T)}$ are the orbital and total single particle momenta, respectively, $m_{P(T)}$ is the projection of $j_{P(T)}$. The dependences of expressions for normalized coefficients $C^{ex}_{l_{P(T)}}$, constants $A_{P(T)}$, $B_{P(T)}$, $D_{P(T)}$, $G_{P(T)}$ and values of $I^0_{PT}(R, L)$ on single particle quantum numbers are given in Appendix. The wave numbers for external and internal parts of the wave function are determined in the following way

$$æ_{P(T)} = \sqrt{\frac{2m}{\hbar^2}\{B_{coul} - E_{P(T)}\}},$$
$$\kappa_{P(T)} = \sqrt{\frac{2m}{\hbar^2}\{E_{P(T)} - \bar{V}_{P(T)}\}},$$



where $\bar{V}_{P(T)}$ is the average value of the single particle potential of light (heavy) nuclei over state $P(T)$, $m$ is the proton mass, $B_{coul}$ is the Coulomb barrier of the nucleus.

The phenomenological and microscopic driving potentials, respectively, calculated by the expressions (3) and (7) for the dinuclear system with $Z_{tot} = 108$ are presented in Figs. 1 and 2. In our microscopic calculation we suppose the $N/Z$-equilibrium in the dinuclear system to be set in the initial stage of reaction. Mass numbers for light nuclei with $Z < 10$ were taken according to the experimental $Q_{gg}$-systematics of isotope production cross sections [4]) for similar reactions. Functional dependence of the microscopic driving potential (7) on the angular momentum is taken into account by the value of the dinuclear system temperature $\tau$.

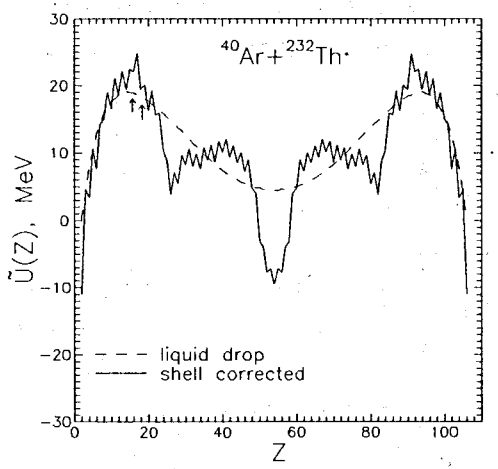


Fig.1. Phenomenological driving potential $U(Z)$ for the system with $Z_{tot} = 108$ and $A_{tot} = 272$ at $\tau = 0$ MeV. The calculated results within liquid drop model are presented by dashed line. The driving potential calculated with use of the real nuclear binding energy in (3) is presented by solid line.

It is seen that the microscopic and macroscopic driving potentials are qualitatively similar. The dependence $\tilde{U}(Z)$ on $Z$ has few local minima. This fact indicates the influence of shell structure on the evolution of the dinuclear system. Absence of the local minima for some magic and even values of $Z$ can be explained by the shell structure of the conjugated nucleus and the influence of the neutron subsystem. It is obvious that the place of the initial configuration defines the evolution direction of the dinuclear system. The driving potential has a minimum at $Z = 16$ and $\tilde{U}(Z = 17) > \tilde{U}(Z = 18) > \tilde{U}(Z = 19)$. Therefore, in the case of $^{40}$Ar+$^{232}$Th reaction the quasifission channel dominates. For the reaction $^{32}$S+$^{238}$U the quasifission and fusion give almost equal contribution to the total cross section. It is to be noted that the microscopic driving potential is sensitive to the mass numbers of the dinuclear system parts. The width of the Businaro-Gallone maximum increases with increasing $N/Z$-

ratio in the light nucleus. For the illustration of this in Fig.3 the calculated microscopic driving potential for the $^{63}$Cu+$^{197}$Au reaction is presented. In this reaction $Z_{tot} = 108$ and $A_{tot} = 260$, that is the system has a smaller numbers of neutrons than in the previous systems.

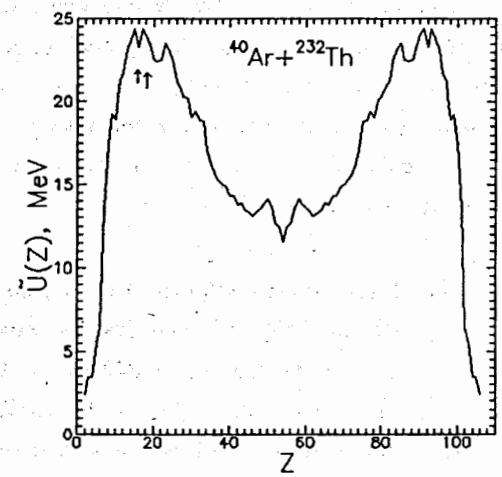


Fig.2. Calculated microscopic driving potential $\tilde{U}(Z)$ for the system with $Z_{tot} = 108$ and $A_{tot} = 272$ ($\tau = 1.0$ MeV and $R = R_P + R_T$). The arrows indicate the injection points for the $^{32}$S(192MeV) +$^{238}$ U and $^{40}$Ar(220MeV) +$^{232}$ Th collisions.

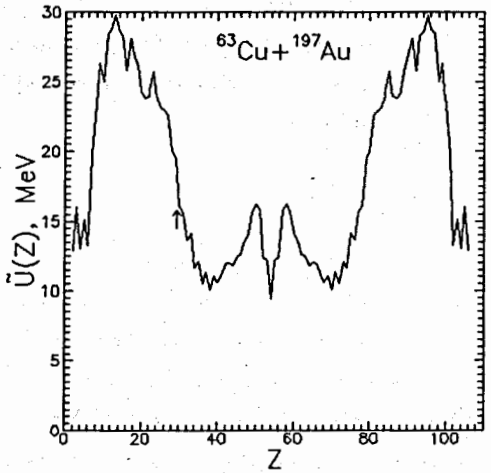


Fig.3. The same as in Fig.2, but for the system with $Z_{tot} = 108$ and $A_{tot} = 272$. The arrow indicate the injection point for the $^{63}$Cu+$^{197}$Au collision.

At the same time the microscopic potential is less sensitive to the increase of the temperature $\tau$. This leads to the weak decrease of the depth of local minima. On the other hand, within the phenomenological model the depths of the local minima decreases fastly with enhancement of $\tau$. Since $\tilde{\Delta}^{(\pm)}_Z - \tilde{\Delta}^{(\pm)}_{Z+1} \sim 1/\tau$ [8]) for near symmetric configurations of the dinuclear system, the influence of the shell structure on the nucleon transfer process decreases less with increasing $\tau$ notwithstanding exponential decrease of the shell correction in the binding nuclear energy. Here it is necessary



to make the following comment. When we speak about shell effects in microscopic consideration, we mean the influence of peculiarities of the single particle spectra near the Fermi surface on the nucleon exchange process. In this approach the concept of the conservation of individuality of the dinuclear system parts plays the key role [12]).

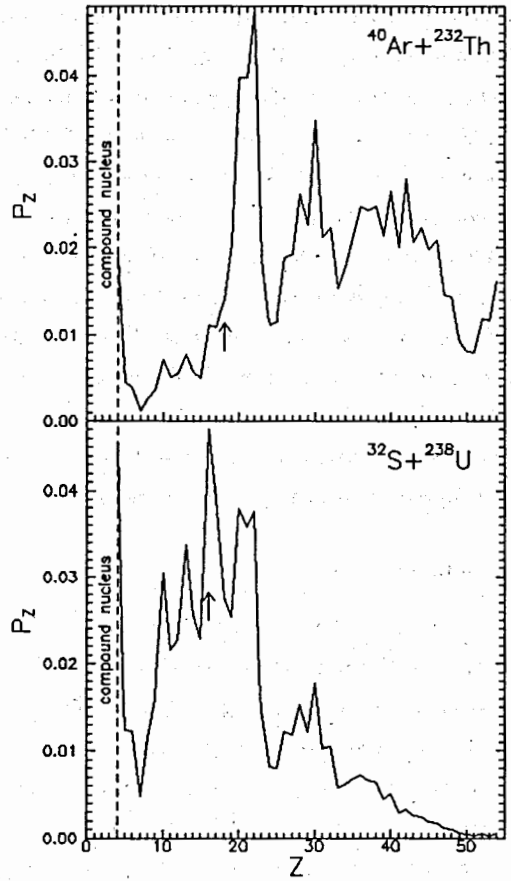


Fig.4. Calculated charge distribution $P_Z$ for the $^{40}$Ar(220MeV)+$^{232}$Th ($\tau = 1.0$ MeV, $R = R_P + R_T$ and $t = 4 \cdot 10^{-21}$s) and $^{32}$S(192MeV) +$^{238}$ U ($\tau = 1.0$ MeV, $R = R_P + R_T$ and $t = 3 \cdot 10^{-21}$s) collisions.

By using the microscopic transport coefficients the calculated charge distributions for the reactions $^{40}$Ar+$^{232}$Th and $^{32}$S+$^{238}$U (Fig. 4) are in good agreement with the experimental data [3,9]). The theoretical dependences give the correct evolution direction for the dinuclear system along the mass asymmetry mode of motion. They reproduce the experimental maxima of the charge distributions and relation between fusion and quasifission channels. This ratio is easily obtained if we consider the dinuclear system motion to more asymmetric forms like the fusion process [12]). The decrease of

asymmetry and decay of near symmetric configurations of the dinuclear system can be considered like quasifission. In the case of $^{32}S+^{238}U$ more than 50% of the cross section correspond to the fusion-fission channel, while about 20% remain in the $^{40}Ar+^{232}Th$ reaction. The other part of the cross section corresponds to the quasifission channel. The discrepancy of the charge (mass) distributions in both reactions can be explained by distinctions of the structure of interacting nuclei in the framework of the microscopic approach. Since the single particle spectra near the Fermi surface of $^{232}Th$ and $^{238}U$ are quite similar, then in the main the shell structure of a light nucleus influences the dinuclear system evolution, that is, the first nonoccupied proton level of $^{32}S$ is quite far from the Fermi surface. This decreases the possibility of the nucleon transfer from a heavy to a light nucleus. On the contrary, $^{40}Ar$ has nonoccupied proton single particle level near the Fermi surface. This stimulates the decrease of the dinuclear system asymmetry. The $N/Z$-ratio in the system influences the ratio of the fusion and quasifission channels as well. For the $^{63}Cu+^{197}Au$ reaction approximately 15% of the cross section corresponds to the increase of the mass asymmetry. This seems to be in a good agreement with experimental results [13].

Thus, in the framework of the microscopic approach it is possible to obtain the qualitative agreement between calculated charge distributions and experimental data.

## 4.Conclusion

Within the microscopic and macroscopic approaches the methods of calculation of the driving potential are very different. Still the calculated results have demonstrated surprising likeness of the microscopic and phenomenological driving potentials. This fact can be considered as further argument for the validity of the microscopic approach based on the concept of the individuality conservation of interacting nuclei. Taking into account the selection rules for change of the angular momentum and its projection within the microscopic variant we obtain the driving potential that carries more information about the ways of the system evolution. This driving potential seems to be more sensitive to the change of the $N/Z$-ratio in the dinuclear system parts.

## Appendix

In the appendix we present the useful expressions for the calculation of the single particle matrix elements $g_{PT}(R)$. In (8) the constants $A_{P(T)}$ are determined in the following form

$$A_{P(T)} = a_{P(T)}\xi(i_{l_{T(P)}}(æ_{P(T)}R_{E_{T(P)}}))$$



where

$$a_{P(T)} = \frac{(E_P + E_T + \hbar^2 æ^2_{P(T)}/m)(æ^2_{T(P)} + \kappa^2_{T(P)})R^2_{E_{T(P)}}}{2(æ^2_{P(T)} + \kappa^2_{T(P)})(æ^2_{P(T)} - æ^2_{T(P)})}$$

$$\xi(f_{l_{P(T)}}(\kappa R_{E_{P(T)}})) = f^2_{l_{P(T)}}(\kappa R_{P(T)})\frac{\partial}{\partial R_{E_{P(T)}}}\left(\frac{k_{l_{P(T)}}(æ_{P(T)}R_{E_{P(T)}})}{f_{l_{P(T)}}(\kappa R_{E_{P(T)}})}\right).$$

Here $f_{l_{P(T)}}(x)$ is one of the spherical Bessel functions.

In (9) constants $B_{P(T)}$, $D_{P(T)}$ and $G_{P(T)}$ have form

$$\begin{aligned} B_{P(T)} = \; & b_{P(T)}[\xi(y_{l_{T(P)}}(\kappa_{P(T)}R_{E_{T(P)}}))\xi(y_{l_{P(T)}}(\kappa_{P(T)}R_{E_{P(T)}})) \\ & -\xi(j_{l_{T(P)}}(\kappa_{P(T)}R_{E_{T(P)}}))\xi(j_{l_{P(T)}}(\kappa_{P(T)}R_{E_{P(T)}}))], \end{aligned}$$

$$\begin{aligned} D_{P(T)} = \; & b_{P(T)}[\xi(j_{l_{T(P)}}(\kappa_{P(T)}R_{E_{T(P)}}))\xi(y_{l_{P(T)}}(\kappa_{P(T)}R_{E_{P(T)}})) \\ & +\xi(y_{l_{T(P)}}(\kappa_{P(T)}R_{E_{T(P)}}))\xi(j_{l_{P(T)}}(\kappa_{P(T)}R_{E_{P(T)}}))], \end{aligned}$$

$$G_{P(T)} = \frac{(-1)^{l_{P(T)}}}{\pi}a_{P(T)}\xi(k_{l_{T(P)}}(æ_{P(T)}R_{E_{T(P)}})),$$

where

$$b_{P(T)} = \frac{\kappa_{P(T)}(E_P + E_T - \hbar^2\kappa^2_{P(T)}/m)(\kappa^2_{T(P)} + æ^2_{T(P)})R^2_{E_P}R^2_{E_T}}{4(\kappa^2_{P(T)} + æ^2_{T(P)})(\kappa^2_{T(P)} - \kappa^2_{P(T)})}.$$

If $æ_P = æ_T$ or $\kappa_P = \kappa_T$ the corresponding limit of (8) or (9) is calculated.

For the normalized coefficients $C^{ex}_{l_{P(T)}}$ we have

$$C^{ex}_{l_{P(T)}} = \sqrt{2}\left[R^3_{E_{P(T)}}\left(1 + \frac{æ^2_{P(T)}}{\kappa^2_{P(T)}}\right)k_{l_{P(T)}+1}(æ_{P(T)}R_{E_{P(T)}})k_{l_{P(T)}-1}(æ_{P(T)}R_{E_{P(T)}})\right]^{-1/2}.$$

So far as in (9) the values of $I^0_{PT}(R,L)$ depend on $R$ weakly and their analytical expression is very complicated, we replaced these terms by their values at $R = R_{E_P} + R_{E_T}$.

## References


1) L.G. Moretto and R.Shmitt, J. Phys. (Paris) **37** (1976) C5-109

2) J.Blocki, J.Randrup, W.Swiatecki and C.F.Tsang, Ann. Phys. (N.Y.) **105** (1977) 427

3) P.Gippner, U.Brosa, H.Feldmeier and R.Schmidt, Phys. Lett. **B252** (1990) 198

4) V.V.Volkov, Phys. Rep. **44** (1978) 93

5) A.N.Mezentsev, A.G.Artukh, G.F.Gridnev, W.Karcz, S.Kliczewski, M.Madeja, V.L.Mikheev, J.Szmiger and V.V.Volkov, Contributed Papers of International Conference on Clustering Aspects in Nuclear and Subnuclear Systems (Kyoto, 1988) 216

6) N.V.Antonenko and R.V.Jolos, Phys. Scr. **T32** (1990) 27

7) N.V.Antonenko and R.V.Jolos, Z. Phys. **A338** (1991) 423

8) N.V.Antonenko and R.V.Jolos, Sov. J. Nucl. Phys. **51** (1990) 690

9) P.Gippner, K.D.Schilling, W.Seidel, F.Stray, E.Will, H.Sodan, S.M. Lukyanov, V.S.Salamatin, Yu.E.Penionzhkevich, G.G.Chubarian and R.Schmidt, Z. Phys. **A325** (1986) 335

10) G.G.Adamian, R.V.Jolos and A.K.Nasirov, Sov. J. Nucl. Phys. **55** (1992) 660

11) M.Abramovitz and J.A.Stegun, Handbook of Mathematical Functions (Nauka, Moskow, 1979) p.254

12) V.V.Volkov, Proc. 6th Int. Conf. on Nuclear Reaction Mechanisms, Varenna, 1991, ed. E.Gadioli (Ricerca Scientifica ed Educazione Permanente, Milano, 1991) p.39

13) B.Jäckel, A.Rox, R.A.Esterlund, W.Westmeier, M.Knaack and P.Patzelt, Z. Phys. **A339** (1991) 475

Received by Publishing Department

on February 14, 1992.